Universiteit Leiden
The Netherlands

Nucleotide excision repair : complexes and complexities : a study of global genome repair in human cells

Volker, Marcel

Citation
Volker, M. (2006, May 15). *Nucleotide excision repair : complexes and complexities : a study of global genome repair in human cells*. Retrieved from https://hdl.handle.net/1887/4390

Version:	Corrected Publisher's Version
License:	Licence agreement concerning inclusion of doctoral thesis in the Institutional Repository of the University of Leiden
Downloaded from:	https://hdl.handle.net/1887/4390

Note: To cite this publication please use the final published version (if applicable).

Chapter 9

The UV-damaged DNA binding protein mediates efficient targeting of the nucleotide excision repair complex to UV-induced photolesions

adapted from
DNA Repair 4, 571–582, May 2005

9 The UV-damaged DNA binding protein mediates efficient targeting of the nucleotide excision repair complex to UV-induced photolesions

Jill Moser,[1] Marcel Volker,[1] Hanneke Kool,[1] Sergei Alekseev,[1] Harry Vrieling,[1] Akira Yasui,[2] Albert A. van Zeeland,[1] Leon H.F. Mullenders[1]

1. Department of Toxicogenetics, Leiden University Medical Center, Wassenaarseweg 72, 2333 AL Leiden
2. Department of Molecular Genetics, Aging and Cancer, Tohoku University, Sendai, Japan

Abstract

Previous studies point to the XPC-hHR23B complex as the principal initiator of global genome nucleotide excision repair (NER) pathway, responsible for the repair of UV-induced cyclobutane pyrimidine dimers (CPD) and 6-4 photoproducts (6-4PP) in human cells. However, the UV-damaged DNA binding protein (UV-DDB) has also been proposed as a damage recognition factor involved in repair of UV-photoproducts, especially CPD. Here, we show in human XP-E cells (UV-DDB deficient) that the incision complex formation at UV-induced lesions was severely diminished in locally damaged nuclear spots. Repair kinetics of CPD and 6-4PP in locally and globally UV-irradiated normal human and XP-E cells demonstrate that UV-DDB can mediate efficient targeting of XPC-hHR23B and other NER factors to 6-4PP. The data is consistent with a mechanism in which UV-DDB forms a stable complex when bound to a 6-4PP, allowing subsequent repair proteins – starting with XPC-hHR23B – to accumulate, and verify the lesion, resulting in efficient 6-4PP repair. These findings suggest that (i) UV-DDB accelerates repair of 6-4PP, and at later time points also CPD, (ii) the fraction of 6-4PP that can be bound by UV-DDB is limited due to its low cellular quantity and fast UV-dependent degradation, and (iii) in the absence of UV-DDB a slow XPC-hHR23B-dependent pathway is capable to repair 6-4PP, and to some extent also CPD.

Keywords: UV-damaged DNA binding protein; Xeroderma pigmentosum group E; 6-4 Photoproducts; Cylcobutane pyrimidine dimmers; Nucleotide excision repair

1 Introduction

The nucleotide excision repair (NER) system is a highly versatile repair pathway capable of removing a wide variety of helix-distorting lesions from genomic DNA. Cyclobutane pyrimidine dimers (CPD) and 6-4 photoproducts (6-4PP), the main products of short-wave ultraviolet (UV) radiation in DNA, are among the lesions processed by NER, and human cells depend solely on NER to repair these UV-photolesions. Defects in genes encoding NER proteins give rise to UV-sensitive disorders, most notably xeroderma pigmentosum (XP), which comprises seven complementation groups (XP-A–XP-G) (1). XP patients are photosensitive and display a strongly elevated risk of developing skin cancers in sunlight-exposed parts of the body.

Biochemically, all XP patients (except XP variants) are found to be defective in global genome repair (GGR), the subpathway of NER capable of removing lesions from the entire genome. In

GGR, a total of ~30 proteins work together to consecutively execute the basic steps that comprise NER: recognition of the DNA damage, unwinding the DNA around the lesion, excision of the oligonucleotide containing the damage and finally resynthesis of the strand using the undamaged template and ligation of the nick (2). Several specialized proteins have been proposed to act in the initial step of damage recognition, including the UV-damaged DNA binding protein (UV-DDB) (3,4), the complex of XPA and replication protein A (RPA) (5,6) and the XPC-hHR23B heterodimer (7). Most recent studies point to the XPC-hHR23B complex as the principle initiator of NER (8,9). However, those studies did not exclude the possibility that in processing certain lesions, e.g. UV-induced photoproducts, the action of XPC-hHR23B in the formation of the incision complex can be preceded by other proteins such as UV-DDB.

UV-DDB is a heterodimer of the p48 and p127 proteins (10), products of the *DDB2* and *DDB1* genes, respectively. Microinjection of purified UV-DDB was originally found to restore the repair defect of XP-E cells as measured by unscheduled DNA synthesis (11). Recently, evidence has accumulated implying that the XP group E phenotype is caused exclusively by mutations in the *DDB2* gene, implicating that the *DDB2* gene corresponds to the *XPE* gene, and p48 to the XPE protein (12–14).

In vitro binding studies have revealed that the UV-DDB protein complex exhibits a high affinity for UV-induced DNA lesions and a moderate affinity for several other types of DNA lesions (3,15–17). Moreover, UV-DDB has an equally high specificity for 6-4PP when compared to the XPC protein, but a much higher affinity for DNA in general (3,16). A high affinity for DNA damage would be consistent with a role for UV-DDB in the recognition of these lesions directly after their infliction. Results of in vitro repair experiments to assess a role of UV-DDB in NER are inconclusive. Extracts from XP-E cells lacking UV-DDB did not show reduced repair of UV-irradiated DNA nor of an oligonucleotide substrate harbouring a single cisplatin lesion when compared to normal human cells (18). Also, the addition of UV-DDB to a reconstituted system stimulated repair only moderately, and even led to inhibition of the reaction at high concentrations (19). In contrast to the abovementioned studies, a recent study by Wakasugi et al. revealed that in their reconstituted repair system using purified factors, the repair efficiency of CPD and 6-4PP was enhanced by UV-DDB, particularly in the case of CPD (20). This result implies that the role of UV-DDB is not limited to repair inside a chromatin context but instead UV-DDB can stimulate repair through direct interaction with the DNA lesion.

Several studies reported that efficient global genome repair of UV damage in vivo did require UV-DDB (4,11,21), suggesting that the protein might be involved in the repair of lesions within a chromatin context. Indeed, p48 shares homology with chromatin reorganising proteins (22) and UV-DDB interacts with the CBP/p300 histone acetyl transferase (23,24), consistent with a function in remodelling of chromatin to allow efficient repair in the vicinity of the lesion.

In vivo studies have shown that p48 and p127 relocalise rapidly to sites containing UV-damaged DNA immediately after irradiation even in the absence of functional XPC protein (20,25). This observation is consistent with a role for UV-DDB in UV damage recognition, even before XPC is involved. However, the impact of the rapid recruitment of UV-DDB to UV damages on the efficiency of NER remains unclear.

Rodent cells efficiently repair 6-4PP, but in marked contrast to humans, show almost no repair of CPD in the genome overall. This marked difference in CPD repair phenotype between human and rodent cells has been attributed to the absence of UV-DDB activity in rodent cells (21). The situation in rodent cells has led to the well-established notion that UV-DDB is essential for repair of CPD by GGR. However, since the affinity of UV-DDB for 6-4PP is considerable higher than

that for CPD (16), UV-DDB might contribute also to GGR of 6-4PP in human cells, the rate of which greatly exceeds that of CPD. Indeed, an XP-E patient with defective repair of 6-4PP was reported (26). In contrast, in other reports repair of 6-4PP in the absence of UV-DDB was either not affected or only delayed (4,21), indicating that XPC-hHR23B by itself is capable of efficiently recognizing and targeting 6-4PP for repair.

In this study, we assessed the NER incision complex formation and repair of 6-4PP in local spots of UV damage, in cells proficient or deficient for UV-DDB. We find that both the accumulation of NER complexes and 6-4PP repair are greatly enhanced in the presence of UV-DDB. Moreover, we present evidence that the cellular quantity of UV-DDB is the limiting factor for this enhanced 6-4PP repair. We propose a mechanism in which UV-DDB accelerates GGR of 6-4PP by binding to the lesion, facilitating the recruitment of XPC and subsequent factors. In the absence of UV-DDB, 6-4PP are repaired by the GGR pathway dependent solely on recognition by XPC-hHR23B, leading to slower but nevertheless complete repair of 6-4PP.

2 Materials and methods

2.1 Cell culture

Primary diploid human fibroblasts used for immunofluorescence studies, derived from a normal individual (VH25) and xeroderma pigmentosum group E patients (XP2RO and XP23PV), were grown in Ham's F10 medium from which hypoxanthie and thymidine were omitted, and supplemented with 15% fetal calf serum and antibiotics at 37°C in a 2.5% CO_2 atmosphere. XP23PV cells were kindly provided by Dr. M. Stefanini (Instituto di Genetica Molecolare, Pavia, Italy). Simian virus 40 (SV40)-immortalized human fibroblasts, wildtype (MRC5) and XP-A (XP12RO), and wildtype Chinese hamster cells (V79B), were cultured under similar conditions in a 5% CO_2 atmosphere. XP12RO cells stably expressing CPD-or 6-4PP photolyase (S. Nakajima and A. Yasui, manuscript in preparation) were kindly provided by Dr. A. Yasui (Nagoya University, Nagoya, Japan). We immortalized fibroblasts derived from a normal individual by telomerase transfection (VH10hTert)(27). Immortilized cells from a XP-E patient (GM01389hTert) were kindly provided by Dr. E.C. Friedberg (University of Texas, Dallas, TX). Both immortilized cells were grown in DMEM supplemented withh 10% fetal calf serum and antibiotics in a 5% CO_2 atmosphere. VH10hTert cells and XP12RO cells expressing photolyases were grown in the presence of 25 µg/ml and 0.5 mg/ml G418, respectively.

2.2 Construction of vectors expressing fusion proteins

Full-length murine *DDB1* cDNA was amplified by PCR using Hot Start GoldStar DNA polymerase (Eurogentec) with the primer set 5-CCG-GAA-TTC-C-GGA-GGC-ATG-TCG-TAC-AAC-TAC-GTC-GT-3′ (forward) and 5-TCC-CCG-CGG-CTA-ATG-GAT-CCG-AGT-TAG-CT-3′ (reverse) and digested with *Eco*RI (forward) and *Sac*II (reverse) endonucleases. The cDNA fragments were cloned in-frame into the *Eco*RI and *Sac*II site of pECFP-C1 (Clontech), resulting in a vector expressing a CFP-p127 fusion protein. Murine *DDB2* cDNA was amplified similarly, using the primers 5-CCG-GAA-TTC-CTC-TTC-ACC-GAG-TAC-GTC-AT-3′ (forward) and 5-CGC-GGA-TCC-CC-GCC-TCC-TAG-TCT-TTC-ATG-ATC-TTT-CT-3′ (reverse). To create a vector expressing p48-YFP fusion protein, after digestion of the cDNA with *Eco*RI and *Bam*HI, the cDNA fragments were cloned in-frame into the *Eco*RI and *Bam*HI site of pEYFPN1 (Clontech). A vector expressing a p48-FLAG fusion protein was created after PCR amplification of murine *DDB2* cDNA using the primer set 5-AT-CCC-AAG-CTT-CTC-TTC-ACC-GAG-TAC-GTC-AT-3′ (forward) and 5-AAG-GAA-AAA-AGC-GGC-CGC-GCT-GCC-ACT-CCT-CAC-AGA-AT-3′ (reverse) and digestion with *Hin*dIII and *Not*I. Resulting cDNA fragments were cloned in-frame into p3XFLAG-CMV (Sigma) at the *Hin*dIII and *Not*I sites to form the p48-FLAG vector, expressing the FLAG polypeptide fused to the C terminus of p48. All vectors contain a *NEO* gene, and a cytomegalovirus promoter to control expression of the fusion genes. After construction of the vectors, all fusion genes were sequenced to ensure that no mutations had been introduced during PCR and cloning.

2.3 Transient transfection of human cells

Immortalised XPA-deficient human fibroblasts stably expressing either CPD-or 6-4PP photolyases were subcultured 24 h before transfection, and subsequently grown in the *absence* of G418 to improve transfection efficiency. Cells were transfected with plasmids p48-YFP and CFP-p127 us-ing the FuGENE6 transfection reagent (Roche Diagnostics) according to the manufacturer's instructions. After transfection, cells were cultured for an additional 24 h to allow expression of the fusion proteins before experiments were carried out.

2.4 Global and local UV irradiation

Confluent cells were washed with phosphate-buffered saline (PBS), irradiated with a Philips TUV lamp (predominantly, 254 nm) at a dose rate of 0.2 W/m^2 as described previously (28). For local UV irradiation, cells on coverslips were washed once with PBS, covered with an isopore polycarbonate filter with pore sizes of 5 or 8 µm (Millipore, Bradford, MA) and UV-irradiated (29). Only half of a coverslip was covered with the filter for experiments with simultaneous local and global UV irradiation. After irradiation, the filter was removed, and cells were returned to culture conditions for times indicated. Photoproducts were removed from the genome of photolyase-expressing cells by exposing the cells for 1 h to light from a far-blue TL tube.

2.5 Antibodies

The following primary antibodies were employed: affinity-purified rabbit IgG polyclonals anti-XPC and antiERCC1, kindly provided by Hanny Odijk and Dr. Wim Vermeulen (Erasmus MC, Rotterdam, The Netherlands); affinity-purified mouse IgG monoclonal anti-RPA70, a gift from Dr. H.P. Nasheuer (National University of Ireland, Galway, Ireland); mouse IgG monoclonals anti-6-4PP and anti-CPD, gifts from Dr. O. Nikaido (Kanazawa University, Kanazawa, Japan); mouse IgG monoclonal anti-XPB, a gift from Dr. J.-M. Egly (IGMC, Illkirch, France); affinity-purified mouse monoclonals anti-XPA and anti-XPG, gifts from Dr. Rick Wood (UPCI, Pittsburg, PA). Secondary antibodies that were utilized are: FITC-conjugated donkey anti-mouse and donkey anti-rabbit IgG; Cy2conjugated goat anti-mouse IgG and goat anti-rabbit IgG; Cy3-conjugated goat anti-rabbit IgG and goat anti-mouse IgG + IgM (Jackson Laboratories, Westgrove, PA). Alexa Fluor 488-conjugated goat anti-mouse IgG was obtained from Molecular Probes (Leiden, The Netherlands). All secondary antibodies were used according to the manufacturer's instructions.

2.6 Fluorescent labelling

The fluorescent labelling was performed essentially as described (9). Briefly, cells were washed twice with cold PBS, fixed and lysed in PBS with 2% formaldehyde and 0.2% Triton X-100 for 15 min on ice and washed again twice with cold PBS. Cells were then incubated with 3% bovine albumin in PBS for 30 min at room temperature. To visualize CPD or 6-4PP, the cellular DNA was denatured with 0.1 M HCl for 10 min at 37^{o}C. Primary and secondary antibodies were incubated for 2 h and 1 h, respectively, at room temperature in washing buffer (WB: PBS, 0.5% bovine albumin, 0.05% Tween-20). After each antibody incubation, cells were washed three times for 5 min with WB. Cells were mounted in Vectashield mounting medium containing DAPI (1.5 µg/ml) (Vector Laboratories, Burlingame, CA) or in Aqua/polymount (Polysciences Inc., Warrington, PA) containing DAPI (1.5 µg/ml) that gave identical results.

2.7 Microscopy and quantification of fluorescent signal

To capture fluorescence images, a Zeiss Axioplan 2 epifluorescence microscope fitted with appropriate filters coupled to an AttoArc HBO 100 W adjustable mercury arc lamp, and a Hamamatsu C5935 cooled CCD camera, were used. The pictures were captured and processed with Metasystems (Altlussheim, Germany) ISIS software. Using the ISIS software package, the total fluorescence intensity of the area to be quantified (whole nuclei or local UV spots) was measured and divided by the surface area, resulting in a specific fluorescence intensity expressed in arbitrary units.

2.8 Gene specific determination of 6-4PP

Cells were grown to confluency in petridishes to ensure that no cells were in S-phase during the experiments. Cells were UV-irradiated with 30 J/m^2, and subsequently incubated in culture medium, and lysed. High-molecular-weight DNA was isolated and purified as described (30). The DNA was restricted with

*Eco*RI, purified and CPD were removed from the DNA by in vitro photoreactivation employing the photolyase derived from *Anacystis nidulans*, kindly provided by Dr. A. Eker (Erasmus University, Rotterdam, The Netherlands) (30). Photoreactivation was checked for completeness by treatment of DNA samples with T4 endonuclease V and subsequent Southern analysis. Equal amounts of DNA (5 µg) were either treated or mock treated with UvrABC excinuclease (2 pmol of each subunit per µgDNA) or 228-UVDE (ultraviolet DNA endonuclease; (31)) endonuclease (5 pmol/µg DNA). UvrABC and 228-UVDE were kindly provided by M. de Ruiter (Leiden University, Leiden, The Netherlands). After incubation, 10 mM EDTA and 0.1% SDS were added and the DNA was purified by phenol and chloroform extraction, precipitated with ethanol and dissolved in TE. The samples were electrophoresed in 0.6% alkaline agarose gels. The DNA was transferred to Hybond N+ membranes by vacuum Southern blotting and hybridised with a ^{32}P-labeled gene-specific probe recognizing both strands of an 18.5 kb *Eco*RI fragment of the human ADA gene (exon 12). Filters were scanned using the Instant Imager (Packard Instrument Company). The number of 64PP per restriction fragment was calculated from the relative band densities of full size restriction fragments in the lanes containing DNA treated or not treated with either UvrABC excinuclease or UVDE endonuclease, using the Poisson expression.

The use of UVDE, a DNA repair enzyme of *Schizosaccharomyces pombe* that cuts at sites of DNA photolesions (31) was introduced in the latter assay to circumvent background cutting in DNA from mock-treated cells, a known property of UvrABC (30). Fig. 2 shows that UVDE does not exhibit non-specific cutting and hence, UVDE provides an important improvement over UvrABC.

3 Results

3.1 Repair of 6–4 photoproducts in normal human and XP-E cells after global UV irradiation

Repair of UV-induced cyclobutane pyrimidine dimers in human cells is dependent on functional p48 based on the results of biochemical and immunochemical analysis of photolesions in normal and XP-E cells (21). Data on repair of 6-4PP in XP-E cells are only available from immunoslotblot analysis and the results are less consistent than for CPD. Most studies failed to detect major differences in rates of 6-4PP repair between p48-proficient and -deficient cells after global irradiation (4,21), whereas a partial repair defect was reported by Itoh et al. (26). We examined the repair of 6-4PP in globally UV exposed normal human and XP-E cells by two different approaches: immunofluorescence and biochemical (gene specific) analysis. Gene specific analysis requires a relative high UV dose (30 J/m^2) to induce a single 6-4PP per gene fragment (30); hence, to allow comparison, both assays were performed with cells exposed to 30 J/m^2. In previous studies, we determined repair of 6-4PP at the gene level with purified UvrABC excinuclease complex to cut at sites of DNA damage (30). Since this report presents the first instance of UVDE endonuclease to replace UvrABC in the DNA cutting reaction, we validated the use of UVDE. First, the initial frequency of 6-4PP observed using UVDE is 0.0196 6-4PP per 10 kb fragment per J/m^2, which is virtually equal to the frequency found with UvrABC (30). Second, we find indistinguishable repair kinetics of 6-4PP in normal human cells when assayed by UVDE or UvrABC (Fig. 1). We assessed the kinetics of 6-4PP repair in normal human fibroblasts (VH25 and VH10hTert) and in human XP-E fibroblasts (XP23PV and GM01389hTert) exposed to 30 J/m^2 of UV light. Autoradiograms of representative experiments and graphs derived from scanning of these autoradiograms are shown in Fig. 2. In normal human cells, 6-4PP are removed fast from both strands of the *Eco*R1 fragment of the *ADA* gene: approximately 70–80% of the 6-4PP are repaired within 4 h and repair is virtually complete after 8 h. This is in agreement with results obtained in our previous studies (30). Furthermore, there is no difference in the kinetics of removal of 6-4PP between normal and

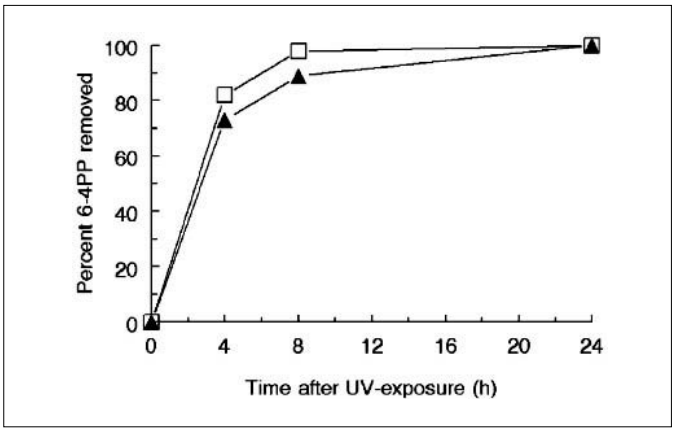

Figure 1. Similar kinetics of 6-4PP repair assayed by UvrABC or UVDE endonuclease
Normal human cells (VH25) were exposed to 30 J/m^2 of global UV. Removal of 6-4PP at various times after irradiation was measured in *Eco*RI restriction fragments of the active *ADA* gene (18.5 kb) using a probe recognising both strands. After photoreactivation of CPD, the DNA was cut using either (□) UvrABC excinuclease or (▲) UVDE endonuclease.

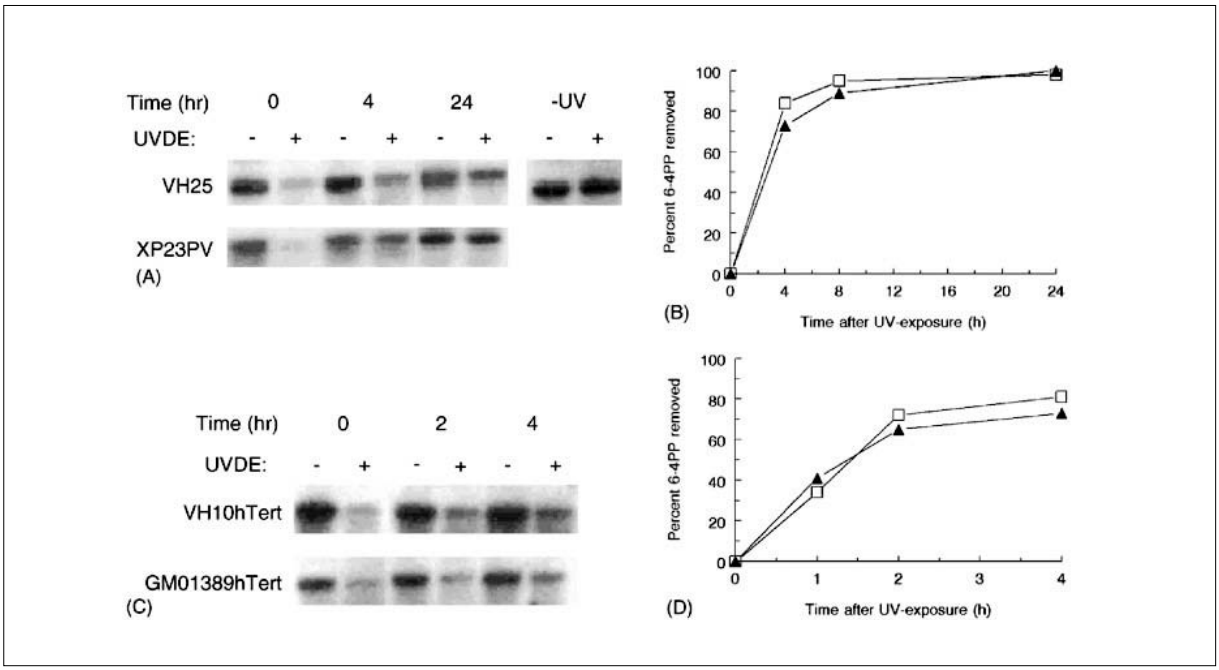

Figure 2. Normal human and XP-E cells repair 6-4PP with similar kinetics after global exposure to 30 J/m^2 UV-radiation, as determined by gene-specific analysis
Removal of 6-4PP at various times after irradiation was measured in EcoRI restriction fragments of the active ADA gene using a probe recognising both strands. After in vitro photoreactivation of CPD, the DNA was cut using the UVDE endonuclease. (A) Autoradiogram and (B) line graph showing removal of 6-4PP over a period of 24 h in (▲) primary normal human (VH25) fibroblasts and (□) primary XP-E (XP23PV) fibroblasts. (C) Autoradiogram and (D) line graph showing removal of 6-4PP over a period of 4 h in (▲) normal human hTert-immortalised fibroblasts (VH10hTert) and (□) XP-E hTert-immortalised cells.

XP-E cells. Also, 6-4PP repair at 4 h observed in primary human fibroblasts (VH25) and in hTert immortalised human fibroblasts (VH10hTert) were not different, which is in line with the observation made by Ouelette et al. (27) that hTert immortilzed cells (normal as well as XP-E) show the same UV survival as primary cells. Consistent with the findings in these biochemical experiments, immunofluorescence measurements demonstrate similar repair kinetics for 6-4PP in human XP-E fibroblasts and normal human cells after an UV dose of 30 J/m^2 (Fig. 3B and D). We note here that the results concerning repair of 6-4PP after global irradiation obtained by the two methodologies are qualitatively similar, i.e. repair in normal and XP-E cells is the same, but that quantitatively the absolute level of repair after 24 h is rather different as measured by the two methods.

3.2 Distribution of NER proteins in normal human and XP-E cells after local UV irradiation of the nucleus

The absence of clear differences in 6-4PP repair kinetics between normal human and XP-E cells suggests equally efficient incision complex formation in normal and XP-E cells. To test this hypothesis, we applied local UV irradiation to confluent human fibroblasts as described previously (9,29) taking into account that incision complex formation during the first 2 h after UV is predominantly due to repair of 6-4PP (9,31,32) (see also, Fig. 4). The distribution pattern of XPC and RPA in normal human and XP-E cells was analysed before and at various times after local irradiation (30 J/m^2). Without UV exposure, both proteins show a homogeneous distribution and strictly nuclear localization (not shown) as observed previously for NER proteins (9). In normal human cells, both XPC and RPA strongly accumulate in the UV-irradiated areas of the nucleus as fast as 5 min after UV exposure. This accumulation persists at a constant level of intensity up to 1 h after UV before slowly returning to the pre-UV pattern (Fig. 5). Since the changes in spot intensities of RPA with time are essentially similar to those of XPC in all performed experiments, only results of XPC protein are shown. In strong contrast to normal human cells, XP-E cells only display a moderate accumulation of NER proteins at damage spots 5 min after UV, while at later stages (30 min and more) after UV, hardly any accumulation is observed (Fig. 5). This indicates that in the absence of UV-DDB, formation of NER incision complexes is strongly reduced. Other

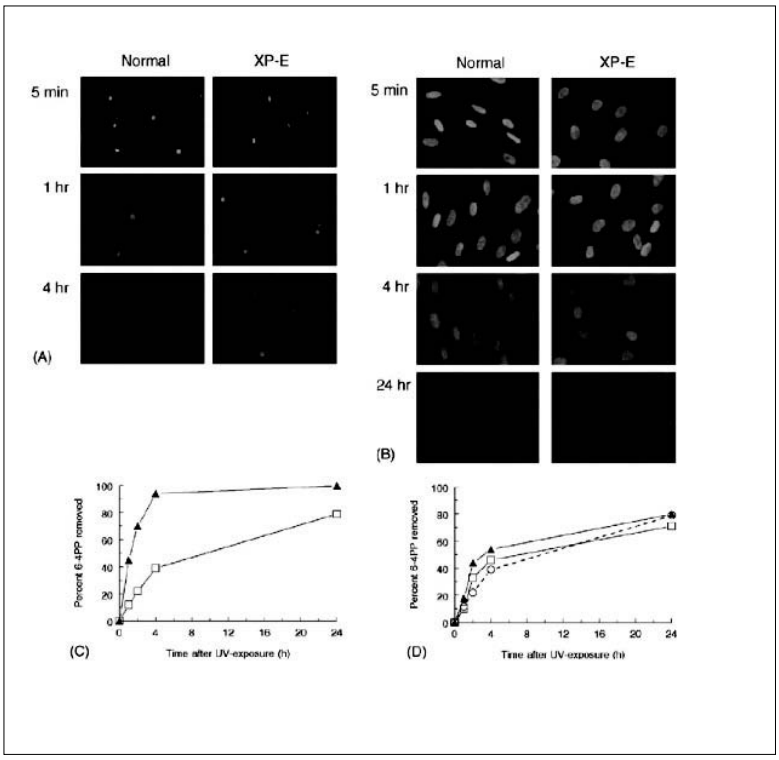

Figure 3. Accelerated 6-4PP repair in normal human fibroblasts (VH10hTert) compared to XP-E fibroblasts (GM01389hTert) after local UV irradiation, but not after global UV irradiation as measured by immunofluorescence
(A) Fluorescent immunostaining of 6-4PP (green) at various times after local UV-irradiation (30 J/m^2) through an 8 µm pore size filter. Images were taken with equal exposure times and merged with DAPI nuclear DNA staining (blue).
(B) Fluorescent immunostaining of 6-4PP (green) at various times after global UV irradiation (30 J/m^2). Images were taken with equal exposure times. (C and D) Graphs presenting the percentage of 6-4PP removed determined from multiple (>20) fluorescent images for each timepoint. (C) Removal of 6-4PP in (▲) normal human and (□) XP-E cells following exposure to 30 J/m^2 of local UV irradiation through an 8 µm pore size filter. (D) Removal of 6-4PP in (▲) normal human and (□) XP-E cells following exposure to 30 J/m^2 of global UV. The dotted line is taken from C showing removal of 6-4PP in XP-E cells which were locally UV-irradiated with 30 J/m^2 and is depicted as a reference. Signal intensities were determined by measuring the total fluorescence intensity of a spot or a nucleus, and dividing by the surface area of the measured spot or nucleus, respectively. See the Appendix for a colour version of this figure.

NER proteins XPA, XPB, XPG and ERCC1 also accumulate only marginally in spots of UV damage after local irradiation of XP-E cells (data not shown), confirming that assembly of the total NER complex is strongly reduced in quantity in the absence of UV-DDB.

Hence, our observations indicate that the complete NER machinery is able to bind to DNA photolesions in the absence of UV-DDB, but that UV-DDB positively affects the kinetics of NER complex formation.

3.3 Effect of UV-DDB on repair of 6-4PP after local UV irradiation of cells

The poor incision complex formation in the absence of UV-DDB conflicts the rather efficient repair of 6-4PP in globally irradiated XP-E cells described in this study and observed by other investigators (4,21). We reasoned that if the level of NER complex accumulation in local UV spots corresponds with the efficiency of 6-4PP repair, the strongly decreased complex formation in XP-E cells implies reduced repair of 6-4PP. Hence, we compared the repair rates of 6-4PP in locally irradiated normal human and XP-E cells at the single cell level using specific antibodies against 6-4PP. To allow direct comparison between globally and locally UV-irradiated cells and to limit experimental variations due to processing for immunofluorescence, about half of the cells on a glass slide were globally exposed whereas the remaining cells were locally irradiated and subsequently processed simultaneously, as described in Section 2.

Consistent with the profound difference in incision complex formation we find that repair of 6-4PP in local spots of UV damage differs greatly between the two cell types. From the data (Fig. 3A and C), it can be deduced that the fluorescent signal for 6-4PP in normal human cells drops rapidly in time, virtually disappearing within 4 h. In striking contrast, 4 h after UV the amount of 6-4PP in XP-E cells is only ~50% reduced compared to the initial levels. We note here that the initial levels of 6-4PP in normal and XP-E cells indicated by the immunofluorescence signal immediately after UV exposure, were virtually the same. The kinetics of accumulation of NER proteins thus coincide with the rate of repair of 6-4PP in local UV spots, strongly supporting the notion that NER complex formation shortly after UV primarily represents recruitment of NER proteins to 6-4PP. This is further supported by the finding that during the first 2 h after UV

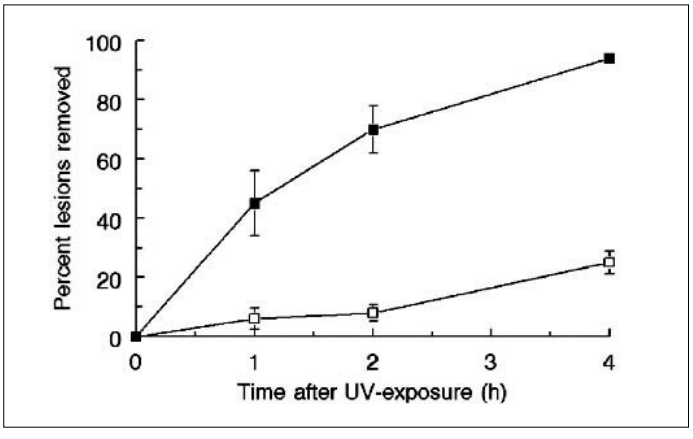

Figure 4. 6-4PP and CPD repair in normal human fibroblasts (VH10hTert) after local UV irradiation through an 8 µm pore size filter with 30 J/m² as measured by immunofluorescence
Cells were immunofluorescently labelled for 6-4PP or CPD at various times following irradiation as described in Section 2. Graphs representing percent repair of 6-4PP (■) or CPD (□) were derived from multiple fluorescent images.

irradiation repair of CPD is strongly lagging behind that of 6-4PP and actually does not amount to more than 8% removal for CPD, compared to 70% for 6-4PP (Fig. 4).

From these findings, we speculated that UV-DDB can mediate the rapid processing of only a limited number of 6-4 photolesions. To test this hypothesis, we irradiated normal human and

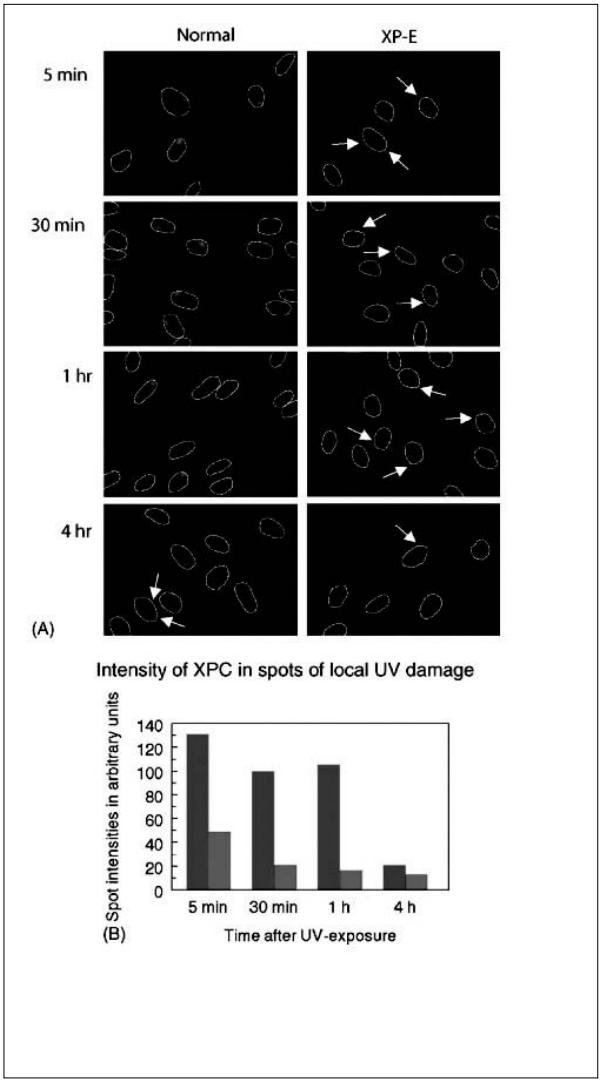

Figure 5. XPC accumulates differentially in normal human fibroblasts (VH10hTert) and XP-E fibroblasts (GM01389hTert) after local UV irradiation
Cells were UV-irradiated with 20 J/m^2 through an 8 µm pore size filter. (A) Fluorescent immunostaining of XPC (red) at various times after irradiation. Arrows indicate protein accumulations in UV-damaged spots that are poorly visible. Dotted lines outline the nuclei as determined from DAPI nuclear counterstaining (images not shown). All fluorescent images were taken with equal exposure times. (B) Bar graph showing average intensities of XPC spots at various time points after irradiation (blue bars: normal cells; red bars: XP-E cells). Spot intensities were determined by measuring the total fluorescence intensity of a spot, divided by its surface area, and corrected for background levels of fluorescence in the nucleus. For each time point, at least 20 cells were measured. The fluorescent signal measured 30 min after UV in normal human cells was set to 100%. See the Appendix for a colour version of this figure.

XP-E cells both locally and globally with a low dose of UV, i.e. 5 J/m^2 and assayed repair of 6-4PP at various times following UV using immunofluorescent labelling of 6-4PP. As shown in Fig. 6, we find that following this low-dose repair kinetics of 6-4PP are more rapid in normal human than in XP-E cells both after local and global UV irradiation. Furthermore, 6-4PP repair in normal human cells is more rapid after local irradiation than after global irradiation, whereas in XP-E cells there is no significant difference between 6-4PP repair kinetics following local or global UV. These results corroborate the idea that UV-DDB does stimulate repair of 6-4PP, but that there is a limit to the number of 6-4PP that can be rapidly repaired through UV-DDB. Interestingly, at this low UV dose, repair of 6-4PP is more rapid in normal human cells after global irradiation than in XP-E cells exposed to local irradiation, despite the fact that in the former situation more lesions are introduced (Fig. 6).

3.4 Distribution of p48 in normal human cells after local UV irradiation of the nucleus

To show that UV-DDB is part of the NER complex that is formed after UV irradiation and, thus, that accumulation of UV-DDB at locally induced UV damage spots follows the same kinetics as other NER proteins, we constructed a human cell line (MRC5) stably expressing p48-YFP. A

similar approach has been successfully applied by Fitch et al. (25,31) to investigate the recruitment of p48 to local damage. The resulting cell line termed MRC5-p48-YFP, expresses p48YFP in >75% of the cells at a moderate to high level (data not shown). Since p127 is present in excess (33), we expect that (following UV irradiation) most if not all p48-YFP to be part of UV-DDB in these cells. The distribution pattern of p48-YFP in unirradiated cells is predominantly nuclear and homogenous, as observed for other NER proteins. After local UV, p48-YFP transiently accumulates at damage spots as observed for other NER proteins such as XPC: intense spots of p48-YFP visible at 30 min after UV, become much weaker in signal 2 h post-UV, and no spots can

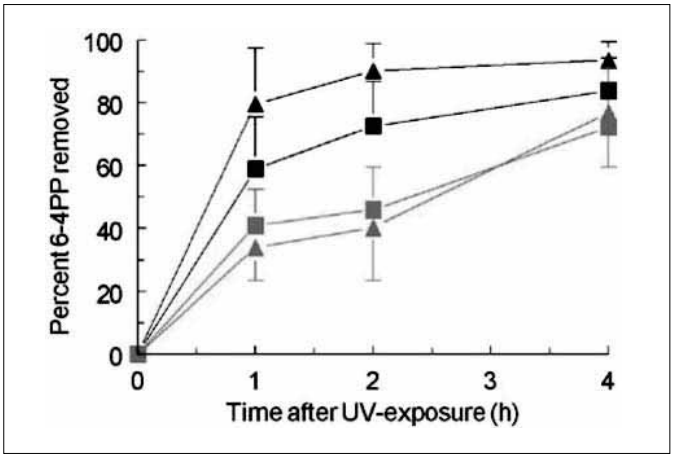

Figure 6. 6-4PP repair in normal human fibroblasts (VH10hTert) and XP-E fibroblasts (GM01389hTert) after local and global UV irradiation with 5 J/m² as measured by immunofluorescence
Cells were immunofluorescently labelled for 6-4PP at various times following irradiation as described in Section 2. Graphs representing percent 6-4PP removed were derived from multiple fluorescent images. Removal of 6-4PP in (black, ■) normal human and (grey, ■) XP-E cells following exposure to global UV. Removal of 6-4PP in (black, ▲) normal human and (grey, ▲) XP-E cells following exposure to UV through an 8 µm pore size filter.

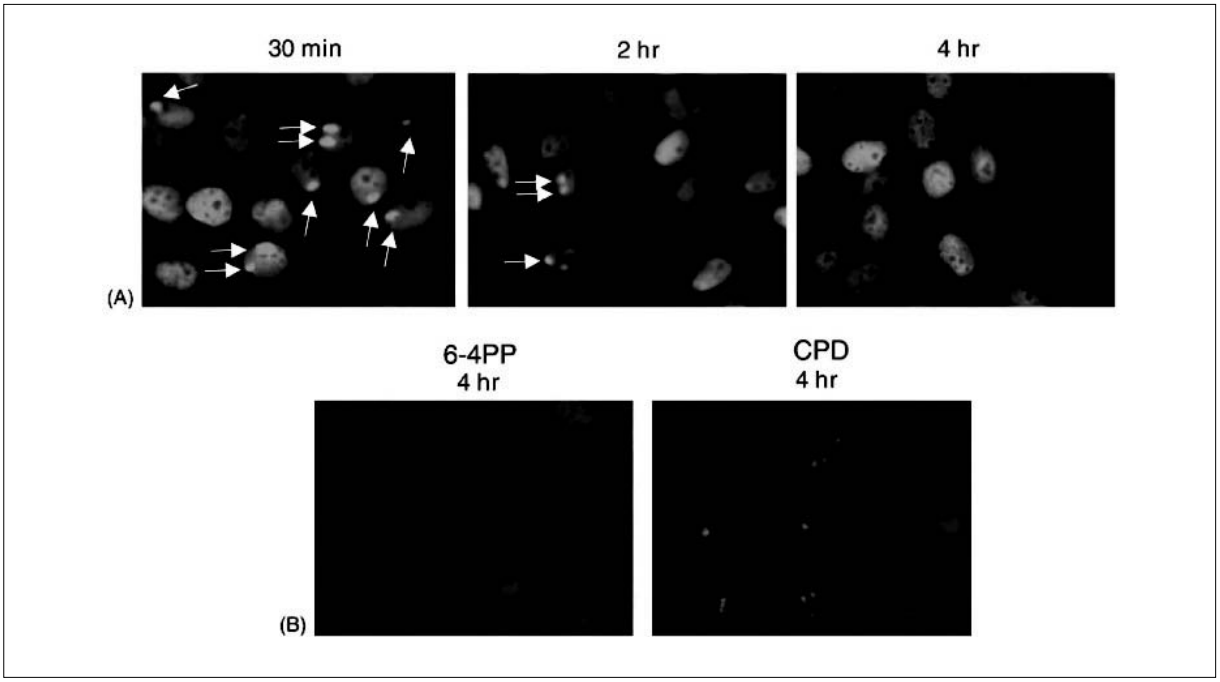

Figure 7. Formation of p48 spots after induction of local UV damage coincides with 6-4PP repair
Normal human cells (MRC5) stably expressing p48-YFP were exposed to 30 J/m² of UV through a 5 µm pore size filter.
(A) Fluorescent images of p48-YFP (green) merged with DAPI nuclear DNA staining (blue) taken at various times following irradiation. Arrows indicate sites of local UV damages. Pictures were taken with equal exposure times. (B) Fluorescent immunostaining using anti-CPD antibody (red) or anti-6-4PP antibody (red) 4 h after exposure, merged with DAPI nuclear DNA staining (blue). See the Appendix for a colour version of this figure.

be detected 4 h after UV (Fig. 7A). At 4 h post-UV, also 6-4PP have become undetectable whereas CPD are clearly detectable in locally irradiated spots (Fig. 7B), indicating that the observed accumulation of p48-YFP in local UV spots mainly takes place at 6-4PP.

To address this point in more detail, we utilized XP-A cells expressing either a CPD or a 6-4PP specific photolyase (referred to as XP-A(CPDpl) and XP-A(6-4pl) cells, respectively). As shown in Fig. 8A, CPD or 6-4PP can be specifically removed by the respective photoreactivating enzyme (25,31) and hence, this system provides an adequate tool to study the relative contribution of either type of photoproduct to the observed accumulation of NER proteins at damage spots. Fig. 8B shows typical results obtained for XPC after photoreactivation of either 6-4PP or CPD in XP-A cells. To estimate the relative affinity of XPC for 6-4PP and CPD in vivo, we utilized images that were captured with equal exposure times. A clearly reduced intensity of XPC spots can be seen when 6-4PP are selectively removed by photoreactivation compared to CPD removal in spite of the fact that CPD are present in three-fold excess over 6-4PP. Similarly, fluorescent staining of p89, the XPB component of TFIIH, also showed a clear signal upon photoreactivation of CPD whereas the signal was virtually absent upon photoreactivation of 6-4PP (data not shown). These observations confirm that 6-4PP are a better substrate than CPD for XPC and UV-DDB to bind to, as previously suggested by Fitch et al. (25,31). In order to visualize the accumulation of p48 and p127 at damage spots, XP-A(CPDpl) and XP-A(6-4pl) cells transiently transfected with both p48-YFP and CFP-p127 were locally UV-irradiated with 30 J/m^2. After removing CPD or 6-4PP by photoreactivation, cells were examined for the distribution of p48-YFP and CFP-p127 as well as immunofluorescently labelled for XPC (Fig. 8C). Under these conditions, accumulations of p48-YFP and CFP-p127 as well as XPC, are observed 1 h after UV when either all CPD or 6-4PP have been removed, suggesting that UV-DDB and XPC accumulate on 6-4PP as well as on CPD under conditions where DDB is overproduced and repair is absent (XPA).

4 Discussion

4.1 NER complex formation at early hours after UV occurs predominantly on 6-4PP

In normal human cells, the signal intensity of p48-YFP in local UV damage spots closely follows the kinetics of 6-4PP repair, in spite of the fact that UV-DDB is essential for repair of CPD in rodent and human cells. This observation suggests that 6-4PP are a stronger recognition signal for UV-DDB than CPD. Indeed, we find shortly (1 h) after irradiation that p48-YFP and CFP-p127, as well as XPC show a pronounced accumulation at 6-4PP in XP-A cells equipped with a photoreactivating enzyme for CPD. In addition, p48-YFP as well as XPC accumulate at UV damage spots in XP-A cells in which 6-4PP were removed by a 6-4PP photolyase. However, in control cells only containing low levels of endogenous p48, the signal of XPC at CPD was much weaker, while the signal of XPB was virtually absent. Fitch et al. (31), employing the same cell system, also observed a higher affinity of UV-DDB for 6-4PP than for CPD in living cells. Furthermore, they observed accumulation of XPC on damage spots in only a minority of cells analysed upon removal of 6-4PP by a photolyase, while ectopically expressed p48 was efficiently recruited to all CPD containing spots. This led them to conclude that p48 is a more efficient recognition factor for CPD than XPC. Although we agree with this statement, we conclude, based on immunostaining of the endogenous XPC protein as well as on the repair kinetics in normal human cells, that 6-4PP are a better substrate than CPD for both XPC and UV-DDB to bind to. Accumulation of both p48 and XPC at CPD in XP-A cells can be observed due to the buildup of incomplete repair complexes. A similar phenomenon is observed in normal human

cells in the presence of inhibitors of repair synthesis (unpublished results). Together, these data provide evidence that UV-DDB stimulates excision repair by direct binding to the lesion as indicated by experiments with a non-chromatin template in vitro (32) and that the accumulation of UV-DDB and other NER proteins observed shortly after local UV predominantly takes place at 6-4PP indicating a functional role of UV-DDB in 6-4PP repair, although UV-DDB also plays a crucial role in repair of CPD.

4.2 UV-DDB mediates accelerated repair of a limited number of 6-4PP

Cells proficient for UV-DDB show a more pronounced accumulation of NER proteins in spots of local UV damage, compared to cells lacking UV-DDB activity, and this enhanced complex formation coincides with an increased repair rate of 6-4PP in local UV spots. Also, after global irradiation with a low dose of UV (5 J/m^2), 6-4PP repair is more rapid in normal human than in XP-E cells. In contrast, after global exposure to a high UV dose (30 J/m^2), we find no significant difference between normal human cells and XP-E cells in the repair kinetics of 6-4PP, i.e. in this situation the accelerating effect of UV-DDB on repair is lost.

We propose the following mechanism to account for these observations. Since we applied equal UV doses in local and global irradiation experiments, the photolesion frequency per unit of DNA is the same in the irradiated areas, and hence the major difference between the

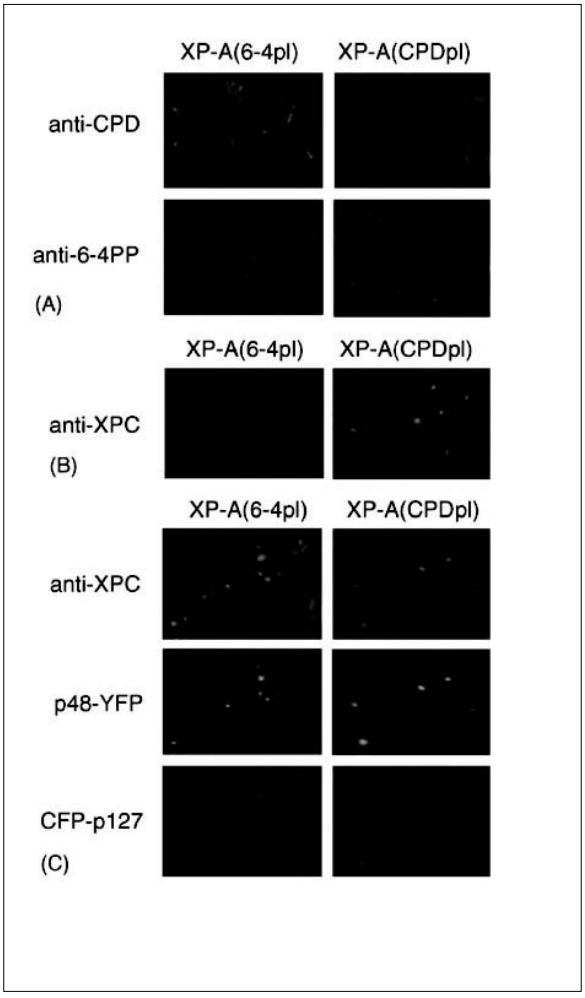

Figure 8. Accumulation of XPC, p48 and p127 in local UV-damaged spots after removal of one of the two types of UV-photolesion by photoreactivation
XP-A cells stably expressing 6-4PP photolyase [XP-A(6-4)phl)] or CPD photolyase [XP-A(CPDphl)], respectively, were irradiated with 30 J/m2 of UV through a 5 µm pore size filter, and exposed to photoreactivating light for 1 h. (A) Fluorescent immunostaining of CPD (red) and 6-4PP (red), merged with DAPI nuclear DNA staining. (B) Fluorescent immunostaining of XPC after photoreactivation of 6-4PP (left) or CPD (right) in XP-A photolyase expressing cells. Pictures taken with equal exposure times and merged with DAPI nuclear counterstaining (blue). (C) XP-A(6-4)phl or XP-A(CPDphl) cells transfected with p48-YFP and CFP-p127 expression constructs 24 h prior to local UV-exposure and 1 h photoreactivation. Fluorescent images of XPC (using anti-XPC antibody, red), p48-YFP (green) and CFP-p127 (blue), taken with exposure times optimised for image clarity. See the Appendix for a colour version of this figure.

two approaches is the total number of lesions introduced per cell. The results imply that the amount of cellular UV-DDB is sufficient to allow enhanced 6-4PP repair after the induction of a (relatively) low number of lesions, i.e. after irradiating locally with 30 J/m^2 or globally with 5 J/m^2, but insufficient to allow rapid repair of the majority of 6-4PP introduced after global irradiation with a high-UV dose. The following calculation corroborates this notion. A dose of 30 J/m^2 of UV-C light introduces approximately 2 × 10^6 CPD (30) in the (diploid) human genome (6 × 10^9 nucleotides). 6-4PP are introduced at one-third of the frequency of CPD, i.e. 7 × 10^5 in total. The typical volume irradiated after local UV through an 8 μm filter encompasses about one sixth of the whole nucleus of a human fibroblast (diameter approximately 20 μm), hence, this volume contains ~10^5 6-4PP. A comparison of the numbers of 6-4PP and the number of UV-DDB molecules, estimated to be ~10^5 (10), shows that after global irradiation with 30 J/m^2 of UV the number of 6-4PP is about seven-fold larger than the number of UV-DDB molecules; whereas, after 30 J/m^2 of local UV, this number is roughly equal. A similar calculation for global UV irradiation with only 5 J/m^2 shows that in that situation too, the number of 6-4PP is approximately the same (~8 × 10^4) as the number of UV-DDB molecules. The most plausible picture of the function of UV-DDB we envisage is that UV-DDB is present in the cell in rate-limiting amounts and is largely consumed during repair of 6-4PP. Moreover, the data suggest that UV-DDB can only function once in the NER reaction and that after recognition of a DNA lesion it becomes inactivated. Such a mechanism is supported by a recent report of Rapic-Otrin et al., who find virtually complete degradation of p48 in primary human fibroblasts in the first 3 h following 15 J/m^2 of UV (24). Other studies (20) reported similar results. As a consequence of this breakdown, most 6-4PP induced after high doses of UV are not repaired with enhanced kinetics through UV-DDB. Yet, the complete removal of 6-4PP from the genome of XP-E cells after global irradiation indicates that these lesions can also be repaired, albeit at reduced rate, through the GGR pathway in which recognition of 6-4PP solely depends on the XPC-hHR23B complex. In contrast, functional UV-DDB is essential for GGR of CPD.

Summarizing, we hypothesize that in vivo (i) 6-4PP can be repaired through a basal mechanism depending only on recognition by XPC-hHR23B; (ii) binding of UV-DDB to 6-4PP will however accelerate their repair; (iii) after binding to a 6-4PP, UV-DDB is degraded and thus cannot assist in subsequent repair of remaining 6-4PP (and CPD). This implies that if 6-4PP are introduced in molar excess to UV-DDB, most 6-4PP will be repaired through direct recognition by XPC-hHR23B, which is a relatively slow process compared to the UV-DDB-stimulated repair mechanism.

4.3 Mechanisms of action of UV-DDB

Several mechanisms might account for a stimulatory effect of UV-DDB on repair of 6-4PP. Binding of UV-DDB to a 6-4PP may result in a structure that facilitates recognition by, and stabilizes binding of subsequent repair components. NER is driven by random diffusion of single components rather than by a pre-assembled repairosome (34–36), i.e. a NER complex will be formed by the consecutive recruitment of proteins. Generally, XPC-hHR23B is assumed to be the crucial factor for initiation of the GGR process (8,9). However, in the absence of UV-DDB the interaction of XPC-hHR23B with a 6-4PP might be relatively weak and frequently subject to dissociation before binding of subsequent factors such as TFIIH, XPA and RPA can stabilize the complex as it is being formed. Consequently, only a few NER incision complexes will be formed to completion.

Two observations provide evidence for this notion. Firstly, the poor accumulation of NER proteins in local UV damage spots in XP-E cells indicates a low steady-state level of NER pre-incision complexes. Secondly, repair of 6-4PP in XP-E cells is equally fast, expressed as percent removed per time unit, after local and global UV irradiation although in the latter situation substantially more lesions are induced.

These results are consistent with a model in which both the general affinity of XPC-hHR23B for DNA and its specific affinity for 6-4PP compared to undamaged DNA is relatively low in vivo. Furthermore, several findings indicate that UV-DDB, in contrast to XPC-hHR23B, is capable of forming a stable complex when bound to a 6-4PP. The general affinity of UV-DDB for DNA is much higher (100–1000-fold) than that of XPC-hHR23B, while the specific affinity for 6-4PP is comparable (3,16). As a result of this high affinity, UV-DDB is the only factor in human whole cell extracts that binds readily to UV-damaged DNA (3). Also, it has been shown that in vivo UV-DDB can bind to photolesions independent of XPC (32). Finally, in UV-DDB-proficient normal human cells we find strong accumulations of NER proteins in local UV-damaged spots and fast repair of 6-4PP. All these data are consistent with the idea that UV-DDB, by virtue of its high affinity for DNA and 6-4PP forms a stable complex when bound to a 6-4PP. This stable state provides subsequent repair proteins – starting with XPC-hHR23B – time to detect and verify the lesion, resulting in efficient 6-4PP repair. The described scenario, in which UV-DDB directly stimulates 6-4PP repair is in agreement with the reported stimulation of 6-4PP repair by UV-DDB in an in vitro repair system employing DNA damage in naked DNA as substrate (20).

Stimulation of 6-4PP repair by UV-DDB might also involve UV-DDB-mediated local chromatin remodelling at sites of photolesions, increasing their accessibility for recognition by XPC-hHR23B. In accordance with a role in chromatin remodelling, p48 has recently been reported to interact with p300/CBP (23,24), while p48 itself bears homology to chromatin-reorganizing proteins (22). Indications that remodelling of chromatin can enhance repair come from recent studies showing that chromatin interacting proteins such as SWI/SNF (37) and HMGN1 (38) enhance NER specifically in the context of chromatin. Moreover, a recent report showed the presence of p48 and p127 together with cullin 4A in a multiprotein complex (the COP 9 signalosome) that possesses ubiquitin ligase activity (39). Not only is this complex a possible candidate to assist in chromatin remodelling by virtue of its combined ubiquitin ligase/UV-damaged chromatin binding activities (38), but also, cullin 4A has been shown to target p48 for ubiquitination and degradation (40).

Finally, UV-DDB might enhance GGR of various types of other lesions for which it displays affinity, such as CPD, *cis*-diamminedichloroplatinum(II) adducts, and nitrogen mustard, among others (3,15) by the same mechanism that accelerates 6-4PP repair.

Acknowledgements

This work was supported by The Netherlands Organization for Scientific Research (ALW) program 'Nucleotide excision repair in its nuclear context' and by European Union Projects nos. QRLT-1999-00181 and MRTN-CT-2003-503618. J. Moser and M. Volker contributed equally to this work. We thank Dr. M. Stefanini (Pavia, Italy) and Dr. E.C. Friedberg (Dallas, TX, USA) for kindly providing cells, Hanny Odijk and Dr. W. Vermeulen (Rotterdam, The Netherlands), Dr. H.P. Nasheuer (Galway, Ireland), Dr. O. Nikaido (Kanazawa, Japan), Dr. J.-M. Egly (Illkirch, France) and Dr. Rick Wood (Pittsburg, PA) for generous gifts of antibodies, and M. de Ruiter (Leiden, The Netherlands) for generously providing UvrABC and UVDE enzymes.

References

1. Bootsma, D., K.H. Kraemer, J.E. Cleaver, and J.H.J. Hoeijmakers, in: 1998). Vogelstein, B., and K.W. Kinzler (Eds.), The Genetic Basis of Human Cancer, McGraw-Hill, New York, pp. 245–74.
2. Laat, W.L. de, N.G. Jaspers, and J.H.J. Hoeijmakers (1999). Molecular mechanism of nucleotide excision repair, Genes Dev. *13*:768–85.
3. Chu, G., and E. Chang (1988). Xeroderma pigmentosum group E cells lack a nuclear factor that binds to damaged DNA, Science *242*:564–7.
4. Tang, J.Y., B.J. Hwang, J.M. Ford, P.C. Hanawalt, and G. Chu (2000). Xeroderma pigmentosum p48 gene enhances global genomic repair and suppresses UV-induced mutagenesis, Mol. Cells *5*:737–44.
5. Asahina, H., I. Kuraoka, M. Shirakawa, E.H. Morita, N. Miura, I. Miyamoto, E. Ohtsuka, Y. Okada, and K. Tanaka (1994). The XPA protein is a zinc metalloprotein with an ability to recognize various kinds of DNA damage, Mutat. Res. *315*:229–37.
6. Li, L., X. Lu, C.A. Peterson, and R.J. Legerski (1995). An interaction between the DNA repair factor XPA and replication protein A appears essential for nucleotide excision repair, Mol. Cell. Biol. *15*:5396–402.
7. Reardon, J.T., D. Mu, and A. Sancar (1996). Overproduction, purification, and characterization of the XPC subunit of the human DNA repair ex-cision nuclease, J. Biol. Chem. *271*:19451–6.
8. Sugasawa, K., J.M. Ng, C. Masutani, S. Iwai, and P.J. van der Spek in: 1998. Eker, A.P., F. Hanaoka, D. Bootsma, and J.H.J. Hoeijmakers
   Xeroderma pigmentosum group C protein complex is the initiator of global genome nucleotide excision repair, Mol. Cells *2*:223–32.
9. Volker, M., M.J. Moné, P. Karmakar, A. van Hoffen, W. Schul, W. Vermeulen, J.H.J. Hoeijmakers, R. van Driel, A.A. van Zeeland, and L.H.F. Mullenders (2001). Sequential assembly of the nucleotide excision repair factors in vivo, Mol. Cells *8*:213–24.
10. Keeney, S., G.J. Chang, and S. Linn (1993). Characterization of a human DNA damage binding protein implicated in xeroderma pigmentosum E, J. Biol. Chem. *268*:21293–300.
11. Keeney, S. A.P. Eker, T. Brody, W. Vermeulen, D. Bootsma, J.H.J. Hoeijmakers, and S. Linn, Correction of the DNA repair defect in xeroderma pigmentosum group E by injection of a DNA damage-binding protein, Proc. Natl. Acad. Sci. U.S.A. *91*:4053–6.
12. Itoh, T., S. Linn, T. Ono, and M. Yamaizumi (2000). Reinvestigation of the classification of five cell strains of xeroderma pigmentosum group E with reclassification of three of them, J. Invest. Dermatol. *114*:1022–9.
13. Itoh, T., and S. Linn (2001). XP43TO, previously classified as xeroderma pigmentosum group E, should be reclassified as xeroderma pigmentosum variant, J. Invest. Dermatol. *117*:1672–4.
14. Rapic-Otrin, V., V. Navazza, T. Nardo, E. Botta, M. McLenigan, D.C. Bisi, A.S. Levine, and M. Stefanini (2003). True XP group E patients have a defective UV-damaged DNA binding protein complex and mutations in DDB2 which reveal the functional domains of its p48 product, Hum. Mol. Genet. *12*:1507–22.
15. Payne, A., and G. Chu (1994). Xeroderma pigmentosum group E binding factor recognizes a broad spectrum of DNA damage, Mutat. Res. *310*:89–102.
16. Batty, D., V. Rapic-Otrin, A.S. Levine, and R.D. Wood (2000). Stable binding of human XPC complex to irradiated DNA confers strong discrimination for damaged sites, J. Mol. Biol. *300*:275–90.
17. Fujiwara, Y., C. Masutani, T. Mizukoshi, J. Kondo, F. Hanaoka, and S. Iwai (1999). Characterization of DNA recognition by the human UV-damaged DNA-binding protein, J. Biol. Chem. *274*:20027–33.
18. Rapic-Otrin, V., L. Kuraoka, T. Nardo, M. McLenigan, A.P. Eker, M. Stefanini, A.S. Levine, and R.D. Wood (1998). Relationship of the xeroderma pigmentosum group E DNA repair defect to the chromatin and DNA binding proteins UV-DDB and replication protein A, Mol. Cell. Biol. *18*:3182–90.

19. Aboussekhra, A., M. Biggerstaff, M.K. Shivji, J.A. Vilpo, V. Moncollin, V.N. Podust, M. Protic, U. Hubscher, J.M. Egly, and R.D. Wood. 1995). Mammalian DNA nucleotide excision repair reconstituted with purified protein components, Cell *80*:859–68.
20. Wakasugi, M., M. Shimizu, H. Morioka, S. Linn, O. Nikaido, T. Matsunaga (2001). Damaged DNA-binding protein DDB stimulates the excision of cyclobutane pyrimidine dimers in vitro in concert with XPA and replication protein A, J. Biol. Chem. *276*:15434–40.
21. Hwang, B.J., J.M. Ford, P.C. Hanawalt, G. Chu (1999). Expression of the p48 xeroderma pigmentosum gene is p53-dependent and is involved in global genomic repair, Proc. Natl. Acad. Sci. U.S.A. *96*:424–8.
22. Hwang, B.J., S. Toering, U. Francke, and G. Chu (1998). p48 Activates a UV-damaged-DNA binding factor and is defective in xeroderma pigmentosum group E cells that lack binding activity, Mol. Cell. Biol. *18*:4391–9.
23. Datta, A., S. Bagchi, A. Nag, P. Shiyanov, G.R. Adami, T. Yoon, and P. Raychaudhuri (2001). The p48 subunit of the damaged-DNA binding protein DDB associates with the CBP/p300 family of histone acetyltransferase, Mutat. Res. *486*:89–97.
24. Rapic-Otrin, V., M.P. McLenigan, D.C. Bisi, M. Gonzalez, and A.S. Levine (2002). Sequential binding of UV DNA damage binding factor and degradation of the p48 subunit as early events after UV irradiation, Nucleic Acids Res. *30*:2588–98.
25. Fitch, M.E., I.V. Cross, and J.M. Ford (2003). p53 responsive nucleotide excision repair gene products p48 and XPC, but not p53, localize to sites of UV irradiation-induced DNA damage, in vivo, Carcinogenesis *24*:843–50.
26. Itoh, T., T. Mori, H. Ohkubo, and M. Yamaizumi (1999). A newly identified patient with clinical xeroderma pigmentosum phenotype has a nonsense mutation in the DDB2 gene and incomplete repair in (6-4) photoproducts, J. Invest. Dermatol. *113*:251–7.
27. Ouellette, M.M., L.D. McDaniel, W.E. Wright, J.W. Shay, and R.A. Schultz (2000). The establishment of telomerase-immortalized cell lines representing human chromosome instability syndromes, Hum. Mol. Genet. *9*:403–11.
28. Venema, J., A. van Hoffen, V. Karcagi, A.T. Natarajan, A.A. van Zeeland, and L.H.F. Mullenders (1991). Xeroderma pigmentosum complementation group C cells remove pyrimidine dimers selectively from the transcribed strand of active genes, Mol. Cell. Biol. *11*:4128–34.
29. Moné, M.J., M. Volker, O. Nikaido, L.H.F. Mullenders, A.A. van Zeeland, P.J. Verschure, E.M. Manders, and R. van Driel (2001). Local UV induced DNA damage in cell nuclei results in local transcription inhibition, EMBO Rep. *2*:1013–7.
30. Hoffen, A. van, J. Venema, R. Meschini, A.A. van Zeeland, and L.H.F. Mullenders (1995). Transcription-coupled repair removes both cyclobutane pyrimidine dimers and 6-4 photoproducts with equal efficiency and in a sequential way from transcribed DNA in xeroderma pigmentosum group C fibroblasts, EMBO J. *14*:360–7.
31. Fitch, M.E., S. Nakajima, A. Yasui, and J.M. Ford (2003). In vivo recruitment of XPC to UV-induced cyclobutane pyrimidine dimers by the *DDB2* gene product, J. Biol. Chem. *278*:46906–10.
32. Wakasugi, M., A. Kawashima, H. Morioka, S. Linn, A. Sancar, T. Mori, O. Nikaido, and T. Matsunaga (2002). DDB accumulates at DNA damage sites immediately after UV irradiation and directly stimulates nucleotide excision repair, J. Biol. Chem. *277*:1637–40.
33. Nichols, A.F., T. Itoh, J.A. Graham, W. Liu, M. Yamaizumi, and S. Linn (2000). Human damage-specific DNA-binding protein p48. Characterization of XPE mutations and regulation following UV irradiation, J. Biol. Chem. *275*:21422–8.
34. Houtsmuller, A.B., S. Rademakers, A.L. Nigg, D. Hoogstraten, J.H.J. Hoeijmakers, and W. Vermeulen (1999). Action of DNA repair endonuclease ERCC1/XPF in living cells, Science *284*:958–61.
35. Hoogstraten, D., A.L. Nigg, H. Heath, L.H.F. Mullenders, R. van Driel, J.H.J. Hoeijmakers, W. Vermeulen, and A.B. Houtsmuller (2002). Rapid switching of TFIIH between RNA polymerase I and II transcription and DNA repair in vivo, Mol. Cells *10*:1163–74.
36. Rademakers, S., M. Volker, D. Hoogstraten, A.L. Nigg, M.J. Moné, A.A. van Zeeland, J.H.J. Hoeijmakers, A.B. Houtsmuller, and W. Vermeulen (2003). Xeroderma pigmentosum group A protein loads as a separate factor onto DNA lesions, Mol. Cell. Biol. *23*:5755– 67.

37. Hara, R., and A. Sancar (2002). The SWI/SNF chromatin-remodeling factor stimulates repair by human excision nuclease in the mononucleosome core particle, Mol. Cell. Biol. *22*:6779–87.
38. Birger, Y., K.L. West, Y.V. Postnikov, J.H. Lim, T. Furusawa, J.P. Wagner, C.S. Laufer, K.H. Kraemer, and M. Bustin (2003). Chromosomal protein HMGN1 enhances the rate of DNA repair in chromatin, EMBO J. *22*:1665–75.
39. Groisman, R., J. Polanowska, I. Kuraoka, J. Sawada, M. Saijo, R. Drapkin, A.F. Kisselev, K. Tanaka, and Y. Nakatani (2003). The ubiquitin ligase activity in the DDB2 and CSA complexes is differentially regulated by the COP9 signalosome in response to DNA damage, Cell *113*:357–67.
40. Nag, A., T. Bondar, S. Shiv, and P. Raychaudhuri (2001). The xeroderma pigmentosum group E gene product DDB2 is a specific target of cullin 4A in mammalian cells, Mol. Cell. Biol. *21*:6738– 47.